

Identification of the Single Specific IQ Motif of Myosin V from Which Calmodulin Dissociates in the Presence of Ca^{2+} †

Hiroshi Koide,[‡] Tatsuya Kinoshita,[‡] Yusuke Tanaka,[‡] Shin'ichiro Tanaka,[‡] Naoki Nagura,[‡]
Gabriele Meyer zu Hörste,[‡] Atsushi Miyagi,[‡] and Toshio Ando*^{‡,§}

*Department of Physics, Kanazawa University, Kakuma-machi, Kanazawa 920-1192, Japan, and
CREST, Japan Science and Technology Agency, Saitama, Japan*

Received July 10, 2006; Revised Manuscript Received July 21, 2006

ABSTRACT: Each heavy chain of dimeric chick brain myosin V (BMV) has a neck domain consisting of six IQ motifs with different amino acid sequences. The six IQ motifs form binding sites for five calmodulin (CaM) molecules and one essential light chain (either 17 or 23 kDa). When the calcium concentration is high, a small fraction of the 10 total CaM molecules dissociates from one molecule of BMV, resulting in loss of actin-based motor activity. At low Ca^{2+} concentrations, two molecules of exogenous CaM associate with one molecule of CaM-released BMV. This suggests that there is a single specific IQ motif responsible for the calcium-induced dissociation of CaM. In this study, we identify the specific IQ motif to be IQ2, the second IQ motif when counted from the N-terminal end of the neck domain. In addition, we showed that the essential light chains do not reside on IQ1 and IQ2. These findings were derived from proteolysis of BMV at high Ca^{2+} concentrations specifically at the neck region and SDS-PAGE analyses of the digests.

Myosin V is a double-headed molecular motor that functions as an organelle transporter in various cells (1–3) and moves processively along actin tracks (4). Myosin V's ATPase kinetics effectively account for the processivity (5–7). The movement proceeds in 36 nm steps (8–10), in a hand-over-hand fashion (11, 12), with the two heads alternating between the leading and trailing positions.

Myosin V consists of two heavy chains and several light chains. The constituent light chains differ between chick brain myosin V (BMV)¹ and murine myosin V. In BMV, each heavy chain is associated with five calmodulin (CaM) light chains, one essential light chain (ELC, either 23 or 17 kDa), and one 8 kDa light chain (identical to the 10 kDa dynein light chain) (13, 14). In murine myosin V, there is a CaM molecule in place of the ELC (7). The heavy chain has an 88 kDa head domain at the N-terminus, adjacent to a neck domain consisting of six IQ motifs of ~24 amino acids each (15), which are the binding sites for CaM and ELC. Next to the neck domain is a coiled coil region that is responsible for dimerization which forms a 30 nm stalk; a globular tail domain lies at the end of the heavy chain.

The motor activity of myosin V is regulated by Ca^{2+} (13, 16). At low Ca^{2+} concentrations ($\text{pCa} > 7.0$), myosin V has full motility, while at high Ca^{2+} concentrations ($\text{pCa} < 6.0$), it has no motility. At high Ca^{2+} concentrations, CaM partially dissociates from the myosin V neck domains (4, 17, 18). Initially, there was disagreement with regard to the potential relationship between CaM dissociation and loss of motor activity (16, 19), but it is now clear that dissociation of CaM greatly weakens the affinity of myosin V for actin, which results in a loss of motor activity (20).

Part of the myosin V neck region that is exposed following CaM dissociation can be refilled with exogenous CaM at low Ca^{2+} concentrations (4). Using exogenous Cy3-labeled CaM, we previously observed that endogenous CaM that had partially dissociated in a relatively high Ca^{2+} concentration solution ($\text{pCa} \sim 5.0$) was replaced with only 2.1 Cy3-labeled CaMs per BMV molecule (4). This was recently confirmed by another group (20). They estimated the number of Cy3-labeled CaM molecules associated with individual myosin V molecules whose endogenous CaM had been substituted with Cy3-labeled CaM at various Ca^{2+} concentrations, using a fluorescence microscope to quantify the number of photobleaching steps. When $\text{pCa} < 5.6$, almost all BMV molecules had two associated Cy3-labeled CaMs, while a very small fraction (<5%) had three associated Cy3-labeled CaMs. These observations suggest that there is a single specific IQ motif responsible for dissociation of CaM from myosin V.

We sought to identify the specific IQ motif. In this study, we demonstrate the following novel findings. (1) At high Ca^{2+} concentrations, proteinase K (PK) specifically cleaves BMV at the neck domain, producing single-headed BMV (S-1) with an exposed IQ motif. (2) The exposed IQ motif

† This study was supported by CREST/JST and a Grant-in-Aid for Basic Research (S) from the Ministry of Education, Culture, Sports, Science and Technology of Japan.

* To whom correspondence should be addressed. E-mail: tando@kenroku.kanazawa-u.ac.jp. Phone: +81 76-264-5663. Fax: +81 76-264-5739.

[‡] Kanazawa University.

[§] CREST, Japan Science and Technology Agency.

¹ Abbreviations: CaM, calmodulin; ELC, essential light chain; RLC, regulatory light chain; BMV, chick brain myosin V; PK, proteinase K; BSA, bovine serum albumin; PMSF, phenylmethanesulfonyl fluoride; EGTA, ethylene bis(oxyethylenetriolo)tetraacetic acid; HMM, heavy meromyosin; S-1, subfragment 1; SDS, sodium dodecyl sulfate; PAGE, polyacrylamide gel electrophoresis.

is refilled with exogenous CaM at low Ca^{2+} concentrations, and the resulting reconstituted S-1 (reS-1) has motor activity. Then, we present analyses of the quantities of CaM in S-1 and reS-1 and successfully identify the single specific IQ motif as IQ2. This conclusion agrees with the previous finding by Trybus et al. that IQ2 is at least one of the sites from which CaM dissociates in Ca^{2+} (16).

MATERIALS AND METHODS

Proteins. BMV was prepared as previously described (21), stored at 0 °C, and used within 10 days. Actin was prepared from rabbit skeletal muscles and purified as previously described (22). Bovine brain CaM, bovine serum albumin (BSA, fraction V), and PK were purchased from Sigma-Aldrich. Streptavidin and casein were obtained from Life Technologies and Nacalai Tesque, respectively.

Ca^{2+} -Induced Dissociation of CaM from BMV. A BMV sample (ca. 100 nM) in a Ca^{2+} -free solution [buffer A containing 100 mM KCl, 20 mM imidazole (pH 7.6), 2 mM MgCl_2 , 1 mM EGTA, and 2 mM 2-mercaptoethanol] was divided into two aliquots. One was cosedimented with F-actin (2 μM), and its pellet was subjected to SDS-PAGE with five different loads to obtain a standard density-load curve. The other was first incubated for 5 min at 25 °C in buffer A and then incubated for 5 min at 25 °C in a Ca^{2+} -containing solution (buffer A containing 1.01 mM CaCl_2). Bound and dissociated CaM were separated by cosedimentation (163000g for 40 min) of BMV with F-actin (2 μM). The pellet and supernatant were subjected to SDS-PAGE, and the ratio of dissociated to bound CaM was estimated from the standard density-load curve.

Digestion of BMV by Proteinase K. BMV was digested with PK using PK:BMV ratios from 1:200 to 1:25 (w/w). BMV (ca. 100 nM) was mixed with PK in buffer A with or without 1.01 mM CaCl_2 and incubated for 10 min at 25 °C. The reaction was quenched by the addition of 100 μM phenylmethanesulfonyl fluoride (PMSF). The digests were subsequently analyzed by SDS-PAGE. Actin-binding components in the samples were separated by cosedimentation with F-actin (163000g for 40 min) and analyzed by SDS-PAGE.

Preparation of BMV S-1, reS-1, and Heavy Meromyosin. BMV (ca. 100 nM) was digested with PK using a 1:40 ratio (w/w) of PK to BMV for 10 min at 25 °C in buffer A with 1.01 mM CaCl_2 . After the reaction had been quenched with the addition of 100 μM PMSF, the sample was placed on ice, mixed with 5 μM F-actin and 2 mM EGTA, and centrifuged at 263000g for 40 min. The pellet was dissolved in a high-ionic strength solution containing 20 mM imidazole (pH 7.6), 600 mM NaCl, 2 mM MgCl_2 , 1 mM EGTA, and 2 mM ATP, and the solution was centrifuged again. S-1 was collected in the supernatant. In the preparation of reS-1, 1 μM CaM or labeled CaM was added to the digested BMV samples at the same time as F-actin and 2 mM EGTA. For measurement of the motor activity of reS-1, the supernatant collected as reS-1 (biotinylated CaM was used) was further purified using a Q-Sepharose column (Amersham Pharmacia Biotech, 5 mm in diameter and 20 mm in length); the supernatant was diluted three times with a solution containing 20 mM imidazole (pH 7.6), 2 mM MgCl_2 , and 1 mM EGTA and loaded on a column equilibrated with buffer B [20 mM

imidazole (pH 7.6), 200 mM NaCl, 2 mM MgCl_2 , 1 mM EGTA, 1 mM 2-mercaptoethanol, and 20 μM PMSF] and 2 mM ATP. After the column was run with buffer B containing ATP and then with buffer B without ATP, reS-1 was eluted with a high-ionic strength solution (200 mM NaCl in buffer B was replaced with 600 mM NaCl). The collected sample was dialyzed against a low-ionic strength solution (200 mM NaCl in buffer B was replaced with 25 mM KCl). BMV heavy meromyosin (HMM; the C-terminal tail domain of BMV is truncated) was prepared in the same way as S-1, except that BMV was digested by PK in the absence of Ca^{2+} . HMM was purified by Q-Sepharose column chromatography in the same way as reS-1.

CaM Labeling. CaM (35 μM) was mixed with 70 μM Cy3 monofunctional *N*-hydroxysuccinimide ester (Amersham Bioscience) or 150 μM biotin-(AC_5)₂ sulfo-OSu (Dojindo Laboratories) in a solution containing 0.3 M KCl, 20 mM boric acid (pH 8.5), and 0.1 mM CaCl_2 and incubated for 1 h at 25 °C. Following the addition of 5 mM dithiothreitol, the samples were exhaustively dialyzed against buffer A to remove unreacted Cy3 or biotin. The amount of incorporated Cy3 was two molecules per CaM, with the amount of Cy3 determined from its absorbance at 550 nm ($\epsilon_{550} = 1.5 \times 10^5 \text{ M}^{-1} \text{ cm}^{-1}$) and CaM concentration determined by the Lowry method. The amount of incorporated biotin was two molecules per CaM, with a biotin concentration determined as described previously (22).

SDS-PAGE. Slab-gel SDS-PAGE was performed using 3% stacking gels and 8 to 16% linear-gradient separation gels. Each sample (50 μL) to be examined was mixed with 25 μL of a SDS-containing sample buffer [0.31 M Tris-HCl (pH 6.8), 30% glycerol, 9.4% SDS, 31% 2-mercaptoethanol, and 0.003% bromophenol blue]. After samples had been run, the gels were stained with a silver staining solution and/or Quick-CBB (Wako Chemicals). For analysis of band intensity, the gels were stained with Quick-CBB alone. Biotinylated CaM in the samples was detected using a property of streptavidin, its persistence to SDS at even a high temperature (25, 26). Each sample was mixed with SDS sample buffer and divided into two aliquots. One (30 μL) was mixed with streptavidin (7 μM , 5 μL) and incubated for 10 min at 35 °C, and the other (30 μL) was mixed with 5 μL of water and incubated for 10 min in boiling water. In the streptavidin-mixed samples, biotin-CaM species migrated in gels as a complex with streptavidin. Each lane in the stained gels was analyzed using analysis software developed in our lab.

In Vitro Actin Filament Sliding Assay. The assay with intact BMV was performed as previously described (4). The assay with reS-1 was performed as follows. A biotin-BSA sample (1 mg/mL, 50 μL) in buffer A was applied to a flow cell (10–20 μL) made from two nitrocellulose-coated cover slips and incubated for 3 min. After the sample had been washed with buffer A, 50 μL of casein (1 mg/mL in buffer A) was placed in the cell, incubated for 3 min, and washed with buffer A. Streptavidin (0.2 mg/mL, 30 μL) in buffer A was applied to the cell, incubated for 3 min, and washed with buffer A. reS-1 reconstituted using biotinylated CaM (ca. 10 nM, 40 μL) was applied to the cell, incubated for 6 min, and washed with buffer A. Rhodamine phalloidine-labeled F-actin (15 nM, 100 μL) was applied to the cell and incubated for 2 min. Last, the buffer solution was replaced with motility buffer containing 2 mM ATP and an oxygen-

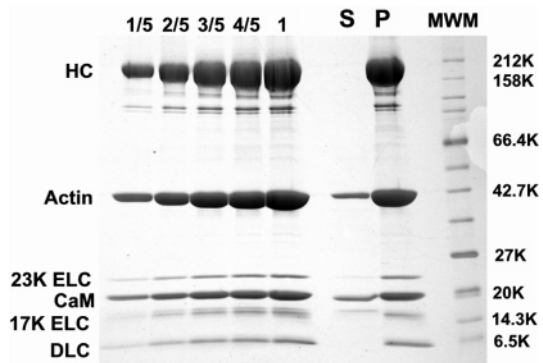


FIGURE 1: SDS-PAGE analysis of the light chain components dissociated or undissociated from BMV at high Ca^{2+} concentrations. BMV incubated at high Ca^{2+} concentrations was cosedimented with F-actin, and its supernatant (S) and pellet (P) were subjected to SDS-PAGE. As a reference for band intensity, myosin V mixed with F-actin at low Ca^{2+} concentrations was also subjected to SDS-PAGE with different loads (from 1/5 to 1). The maximum load (1) is the same as the total load of the pellet and supernatant. HC, myosin V heavy chain; DLC, 10 kDa dynein light chain; MWM, molecular mass markers.

scavenging system (0.2 mg/mL glucose oxidase, 0.36 mg/mL catalase, and 4.4 mg/mL glucose) in buffer A. The sliding movement of actin filaments was observed at 25 °C using an SIT video camera (C2741-08, Hamamatsu Photonics) coupled with an image intensifier (VSA-1845, Video Scope). The image intensifier was connected to a microscope (IX71, Olympus) equipped with an oil-immersion objective (Plan-Apo 100 \times , NA 1.40, Olympus) and an objective lens-type evanescent illumination with a diode green laser (GCL-050-L, 532 nm, Crystal Laser) and a filter set (U-MWG2, Olympus). The image recording and analysis were performed as previously described (4).

Atomic Force Microscopic Imaging. An atomic force microscope (AFM) developed in the lab and nearly the same as that described previously (23, 24) was used. One drop (ca. 1.5 μL) of the purified BMV S-1, reS-1, or HMM (ca. 2 nM) was placed on freshly cleaved mica (1 mm in diameter) for 3 min, rinsed with buffer A, and imaged in a solution containing 20 mM KCl, 25 mM imidazole (pH 7.6), 2 mM MgCl_2 , and 1 mM EGTA.

RESULTS

Quantity of Dissociated CaM. It was previously reported that approximately three CaM molecules (ca. 30% of the total of 10 CaMs) dissociated from one molecule of BMV in Ca^{2+} (17). The number was reported to be approximately two with mouse myosin V constructs having two or six IQ motifs (19). On the other hand, the number of exogenous CaMs (Cy3-labeled CaMs) incorporated into partially CaM dissociated BMV was reported to be two per BMV (4); this number was recently confirmed by the fluorescence microscopic observation of individual BMV molecules with Cy3-labeled CaM (20). Although the number of released CaMs need not necessarily equal the number of incorporated exogenous CaMs, it is more likely that this is so. Here we re-examine the number of dissociated CaMs by separating bound and free CaMs using an actin cosedimentation method. As shown in Figure 1, addition of Ca^{2+} resulted in partial dissociation of CaM from the heavy chain. The densities of CaM in the supernatant and pellet were the same (within

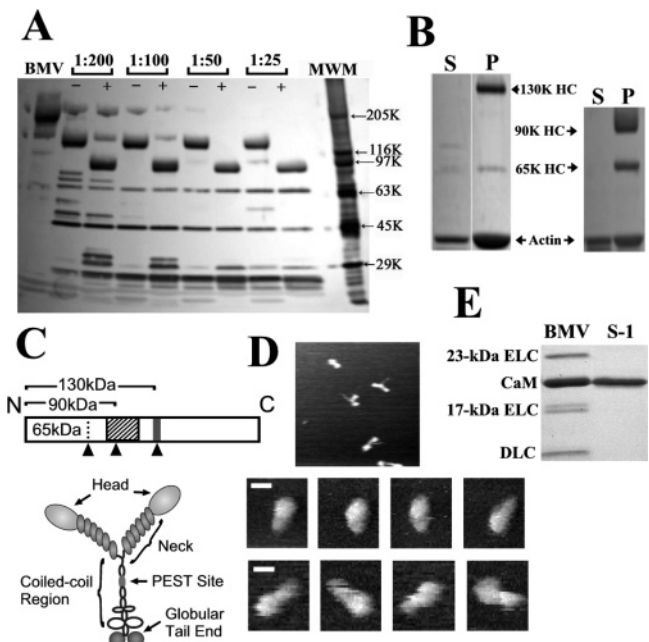


FIGURE 2: SDS-PAGE analysis of cleavage of myosin V by PK in the presence or absence of Ca^{2+} . (A) Cleavage patterns as a function of the weight ratio of PK to BMV and the presence of Ca^{2+} . The weight ratio is indicated at the top. The left lane (marked with BMV) contained intact BMV. The marks + and - at the top indicate the presence and absence, respectively, of Ca^{2+} during proteolysis. The right lane contained molecular mass markers (MWM). (B) Separation by cosedimentation with F-actin of actin-binding and nonbinding components of the digests obtained in the absence (left) or presence (right) of Ca^{2+} . S denotes supernatant and P pellet. (C) Stick diagram of the myosin V heavy chain and sketch of myosin V. In the stick diagram, the dotted line represents a junction corresponding to the 50 kDa/20 kDa junction of conventional myosin II. The shaded portion and gray bar represent the IQ motifs and PEST site, respectively. The arrowheads denote the PK cleavage sites. (D) AFM images of actin-binding fractions. The top image (scan range, 250 nm) is a sample obtained with cleavage of BMV by PK in the absence of Ca^{2+} (i.e., HMM); the image library in the middle line (scale bar, 10 nm) was obtained with S-1 (a sample obtained with cleavage of BMV by PK in the presence of Ca^{2+}), and the image library in the bottom line (scale bar, 10 nm) was obtained with reS-1. (E) Light chain components contained in BMV and S-1 obtained by cleavage of BMV by PK in the presence of Ca^{2+} . The faint band just above the 17 kDa ELC (left lane) is not identified. DLC is the dynein 10 kDa light chain. The amounts of CaM contained in the loaded BMV and S-1 are approximately the same (i.e., the number of moles of S-1 loaded is ~5 times more than that of BMV).

$\pm 10\%$) as that of the BMV samples whose loaded amounts were one-fifth or four-fifth, respectively, of the total load (pellet and supernatant) of the Ca^{2+} -treated sample. Thus, these analyses indicate that approximately two CaMs per BMV were released. Therefore, we can conclude that the number of released endogenous CaMs is approximately equal to the number of incorporated exogenous CaMs. Figure 1 additionally showed that there were two bands around 17 kDa, and the top band (fainter band) appeared in the supernatant and did not appear almost completely in the pellet. Although at present we cannot identify this Ca^{2+} -sensitive light chain, there is a possibility that it is a regulatory light chain (RLC).

PK Digestion of BMV. Digestion of BMV with PK in the absence of Ca^{2+} yielded primarily a 130 kDa fragment (Figure 2A). The amounts of the other fragments diminished with an increasing amount of PK, with the exception of the

65 kDa fragment, the amount of which slightly increased. The 130 and 65 kDa domains demonstrated F-actin binding (Figure 2B, left panel). These fragments' molecular masses and F-actin binding properties are very similar to those produced by calpain digestion of BMV in the presence of Ca^{2+} (17). On the basis of the previously reported analysis (17) of calpain-digested BMV fragments, we understand the 130 kDa fragment to be the N-terminal half of myosin V digested at (or near) the PEST site and the 65 kDa fragment to be the N-terminal head domain fragment (see Figure 2C). The cleavage site that produces the 65 kDa fragment corresponds to the 50 kDa/20 kDa junction of conventional myosin II, and the 65 kDa fragment is associated with a fragment containing a neck domain (17).

On the other hand, PK digestion in the presence of Ca^{2+} yielded primarily a 90 kDa fragment (Figure 2A). This domain also demonstrated F-actin binding (Figure 2B, right panel). On the basis of these results and the fact that Ca^{2+} induces dissociation of two CaMs from one BMV molecule, we take the 90 kDa fragment to be the N-terminal head domain with a neck domain fragment (i.e., a heavy chain of BMV S-1) that is produced by cleavage of the neck domain, likely at the exposed IQ motif. The AFM images (Figure 2D) of the actin-binding fractions produced by digestion at low or high Ca^{2+} concentrations seem to support this interpretation. The fraction obtained at low Ca^{2+} concentrations revealed a two-headed structure with a short tail (Figure 2D, top image), while the fraction obtained at high Ca^{2+} concentrations revealed a single-headed structure with a globular head domain associated with a short neck (Figure 2D, middle line). SDS-PAGE of the S-1 fraction purified by cosedimentation with F-actin indicated that S-1 did not contain ELC at all but instead CaM (Figure 2E). The apparent molecular mass of the S-1 heavy chain, 90 kDa, suggests that the neck domain may contain only IQ1 [on the basis of the amino acid sequence (15), the molecular mass of such an N-terminal heavy chain is calculated to be 91.5 kDa]. Although the validity of this inference is uncertain, it is very certain that the light chain associated with IQ1 is CaM and not ELC.

Reassociation of CaM and S-1. After partial dissociation of CaM at $\text{pCa} < 5.6$, BMV can reassociate with two exogenous CaM molecules at low Ca^{2+} concentrations (4, 20). We examined whether this property persists with BMV S-1. Cy3-labeled CaM and EGTA were added to BMV digested with PK in the presence of Ca^{2+} , and the sample was copelleted with F-actin. The composition of the pellet was analyzed by SDS-PAGE, and surprisingly, Cy3-labeled CaM was found in the pellet (Figure 3). This finding indicates that S-1 possesses an exposed IQ motif fragment that still retains an (almost) complete sequence of the original IQ motif and therefore the ability to bind CaM. This means that PK digests the heavy chain at (or near) the junction between the exposed IQ motif and the next IQ motif on the C-terminal side. The AFM images of reS-1 (Figure 2D, bottom line) revealed a structure different from S-1 (Figure 2D, middle line); the globular head domain looked similar, but the neck region was approximately 2 times longer than that of S-1.

To examine if reS-1 possesses motor function, an *in vitro* actin filament gliding assay was performed, using exogenous biotinylated CaM, and the resulting reS-1 was being adhered to a streptavidin-coated glass surface. The reS-1 retained

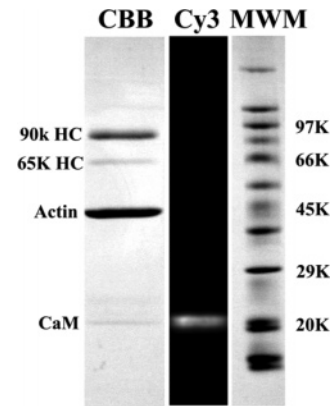


FIGURE 3: SDS-PAGE analysis of incorporation of Cy3-labeled CaM into BMV S-1. Cys3-labeled CaM, F-actin, and EGTA were added to BMV digests obtained in the presence of Ca^{2+} and then centrifuged. The pellets were analyzed by SDS-PAGE. The left lane is a Quick CBB-stained gel and the center lane a fluorescence image of the unstained gel, and the right lane contained molecular mass markers.

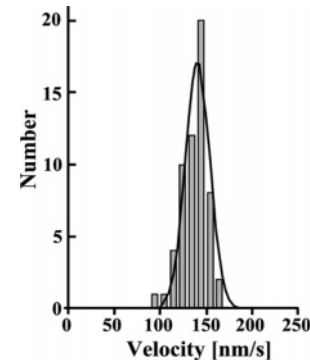


FIGURE 4: Histogram of the speed of actin filament sliding propelled by reS-1 reconstructed using biotinylated CaM.

motor function, and the sliding speed of actin filaments was 140 nm/s (Figure 4), one-fourth of that with BMV (560 nm/s) under similar conditions.

Identification of a Single, Specific IQ Motif. It was difficult to accurately determine the concentrations of the purified S-1 or reS-1, because they were quite low (<100 nM). Therefore, we could not directly determine the number of CaMs contained in S-1 or reS-1. However, only one endogenous CaM can dissociate, and only one exogenous CaM can reassociate with one heavy chain. On the basis of this fact, from the ratio (r) of the amount of CaM contained in S-1 to that in reS-1, we could determine the number (N) of CaMs contained in one molecule of reS-1 [$N = 1/(1 - r)$] and use it to determine the single, specific IQ motif from which CaM dissociates at high Ca^{2+} concentrations. First, we analyzed SDS-PAGE of S-1 and reS-1 to compare the band densities of the 90 kDa heavy chain fragment and CaM (Figure 5A). Although the concentration difference between the two samples was very small, it was compensated using the 90 kDa band densities to determine the ratio r . Analysis of SDS-PAGE with three separate sample preparations resulted in an average r of 0.43, which gave an N of 1.8. Next, we analyzed SDS-PAGE of only reS-1 (reconstituted using biotinylated CaM) mixed or unmixed with streptavidin (Figure 5B). In this case, the concentrations of the two samples were nearly identical. Prior to the performance of SDS-PAGE, the sample mixed with streptavidin was

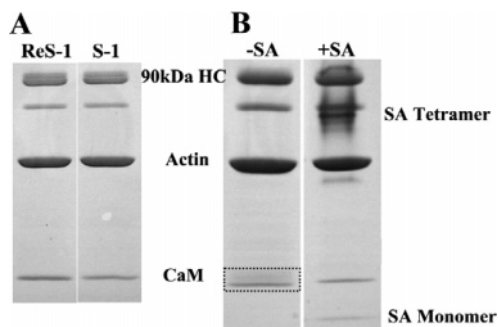


FIGURE 5: SDS-PAGE analysis of the amounts of CaM that are contained in S-1 and reS-1. (A) The sample is a suspension of the pellet obtained by centrifuging a mixture of F-actin and S-1 or reS-1. The left lane contained reS-1 reconstituted using nonlabeled CaM and right lane S-1. (B) The sample was reconstituted using biotinylated CaM. For the left lane, the sample in SDS sample buffer was heated at 100 °C for 10 min, and for the right lane, the sample mixed with streptavidin (SA) in SDS sample buffer was incubated at 35 °C for 10 min.

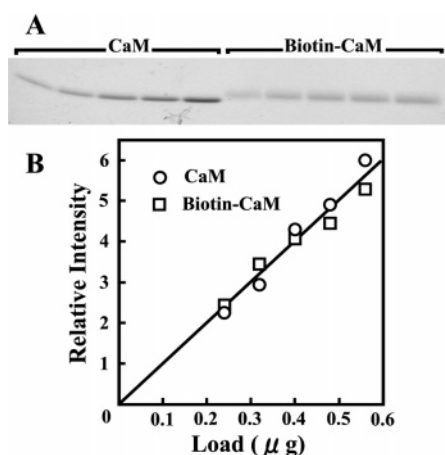


FIGURE 6: (A) Difference in migration on the gel between nonlabeled CaM (left five lanes) and biotinylated CaM (right five lanes). These samples in SDS sample buffer were heated in boiling water for 10 min. (B) The integrated band densities as a function of load for nonlabeled CaM (○) and biotinylated CaM (□). This analysis was performed for the gel shown in panel A.

incubated in SDS sample buffer for 10 min at 35 °C. Streptavidin incubated in SDS at even 70 °C retains its tetrameric structure and an ability to bind to biotin (25, 26). CaM unfolded in SDS at a temperature as low as 35 °C and migrated on SDS-PAGE at the same rate as CaM heated at 100 °C (the sample not mixed with streptavidin was incubated in boiling water). The reS-1 not mixed with streptavidin showed a sharp CaM band, with a blurred band situated just above (Figure 5B, left lane). This blurred band was identified as biotinylated CaM (Figure 6A). Even with such blurred bands, the integrated band densities were quantitatively similar to those of sharp bands of nonlabeled CaM (Figure 6B). Therefore, the region surrounded by a rectangle shown in the left lane of Figure 5B was analyzed to derive the total amount of CaM contained in the reS-1 sample. On the other hand, the reS-1 mixed with streptavidin did not exhibit such a blurred band just above a sharp CaM band (Figure 5B, right lane), indicative of binding of biotinylated CaM to streptavidin in the gel. The mean ratio (over five separate sample preparations), r , was 0.47 ± 0.03 , similar to the result from the previous analysis (0.43). A ratio

of 0.47 results in an N of 1.9. On the basis of these analyses, we conclude that the single, specific IQ motif is IQ2.

DISCUSSION

In the presence of 2 mM CaCl_2 , digestion of BMV with a calcium-dependent cysteine peptidase, calpain, yields actin binding fragments (130 and 65 kDa) and an 80 kDa tail fragment (17). The cleavage sites of the heavy chain are located one amino acid from the PEST site and within the head domain (equivalent to the 50 kDa/20 kDa junction in conventional myosins). Judging from their molecular masses, these cleavage sites are very similar to those cleaved by a serine endopeptidase (PK) in the absence of Ca^{2+} ($\text{pCa} > 7$). From the above result with calpain digestion of BMV in Ca^{2+} , the neck region exposed due to CaM dissociation does not seem to have such a flexible structure that is susceptible to proteolytic cleavage. However, in this study, we found that digestion of BMV with PK yielded an actin-binding 90 kDa fragment only in the presence of Ca^{2+} . The resulting S-1 still retained the ability to bind to exogenous CaM, suggesting that the exposed, specific IQ motif is intact following proteolysis and that the cleavage site must be situated very near the junction between the specific IQ motif (IQ N) and the next IQ motif (i.e., IQ $N+1$). Dissociation of CaM from the specific IQ motif may affect the neighboring CaM or ELC in a way that the junction region may be forced to assume a flexible structure susceptible to cleavage by PK. Alternatively, binding of Ca^{2+} to CaM that has attached to IQ $N+1$ may move the CaM toward IQ $N+2$, thus further exposing the junction region, which is then attacked by PK. It has recently been suggested by Martin and Bayley (27, 28) that such movement of CaM likely takes place in response to the binding of a Ca^{2+} -saturated CaM to two adjacent IQ motifs (i.e., bridge formation). PK has a very broad cleavage specificity. It cleaves peptide bonds adjacent to the carboxylic group of aliphatic and aromatic amino acids. Because of its very broad specificity, we cannot precisely localize the cleavage site that produced the 90 kDa fragment.

We here identify the single, specific IQ motif from which CaM dissociates at high Ca^{2+} concentrations as IQ2. This finding seems consistent with the AFM images of S-1 and reS-1 (Figure D) and with previously reported results (16, 28, 29). The affinity of CaM for six separate peptides (IQ1–IQ6 sequences from murine myosin V) varies and depends on the presence of Ca^{2+} (28). At low Ca^{2+} concentrations, the IQ2 peptide has the lowest affinity for CaM (dissociation constant of $\sim 1.6 \mu\text{M}$), while the dissociation constants with the other IQ peptides are 1–2 orders of magnitude smaller. An increasing Ca^{2+} concentration enhances the affinity of CaM for IQ3–IQ6, while the affinity for IQ1 slightly decreases. In contrast to these changes, the affinity of CaM for IQ2 significantly decreases (dissociation constant of $\sim 13 \mu\text{M}$). In addition, a monomeric murine myosin V construct composed of the motor domain and two IQ motifs (IQ1 and IQ2) partially releases CaM in the presence of Ca^{2+} , while a construct with one IQ motif (IQ1) retains CaM both in the presence and in the absence of Ca^{2+} (16, 29). However, there are reports that do not seem to agree with our view of dissociation of CaM from only IQ2 (30–32). Sakamoto et al. (30, 31) were able to exchange CaM into the 2IQ HMM construct from murine myosin V even though it contains IQ1 and IQ6 in this order. Since CaM does not dissociate from

IQ1 (16), the exchange must have occurred at IQ6. However, the affinity of Ca^{2+} -saturated CaM for each IQ motif depends on the neighboring IQ motifs, because one CaM molecule can bind to double-length IQ sequences (i.e., bridging) (27, 28). Therefore, it is plausible that the affinity of CaM for IQ6 in IQ1–IQ6 would be much lower than that for IQ6 in natural IQ5 and IQ6. Yildiz et al. (32) observed stepwise movement of myosin V along actin tracks, in which the endogenous CaM was partially replaced with fluorescently labeled CaM so that fewer than one fluorophore could be introduced into each myosin V molecule. A constant step size of 74 nm was mainly observed. In some cases, alternative steps of 52 and 23 nm, or 42 and 33 nm, were observed, indicating that several IQ motifs contain exchangeable CaM. However, the maximum number of exchangeable CaMs is reported to be three per myosin V, although the maximum exchange occurs with a small probability (<5%) (20). Therefore, the alternative steps with different sizes must have been observed with such a small probability and do not contradict our conclusion.

In this study, we did not seek to identify the light chain that appeared just above the 17 kDa ELC on SDS–PAGE and dissociated almost completely from myosin V in Ca^{2+} . In previous studies, its existence was not recognized, because of its very small quantity. On the basis of its Ca^{2+} sensitivity and molecular mass (~ 18 kDa), the unidentified light chain may be a regulatory light chain (RLC). Its quantity is much smaller than the amount of ELCs, and therefore, only a small fraction of BMV contains the light chain. We showed that ELCs do not reside on either IQ1 or IQ2. However, ELCs as well as CaM can bind to IQ1 when the 11Q S-1 construct (containing IQ1) from BMV was coexpressed with one of the non-muscle myosin ELC isoforms (either LC-1sa, truncated LC-1sa, or LC-17b) or CaM (33). From the coexpression with two ELC isoforms or with one ELC isoform and CaM, the relative order of affinity for the IQ1 is suggested to be as follows: LC-1sa > LC-17b > CaM. However, differences in the expressed amounts of these light chains are not reported. Kinetic parameters of acto-myosin V ATPase reaction are not strongly influenced by the light chain isoforms, except for the K_m for actin (i.e., the actin concentration at the half-maximal ATPase rate). Because of this small influence on the kinetics, the crystal structure of the myosin V head determined using the 11Q S-1 construct with LC-1sa (34) may not be so different from the structure of S-1 with the native complement of CaM.

It is intriguing that IQ2 mediates Ca^{2+} regulation of myosin V motor function. Release of CaM from IQ1 might significantly affect the structure of the motor domain, which would lead to irreversible change. If Ca^{2+} induced dissociation of CaM from IQ3 or one of the more distant IQ motifs, there might be little effect on the motor domain structure or motor function. Thus, it appears that IQ2 has necessarily been naturally selected. A situation similar to this occurs in a scallop myosin that shows myosin-linked Ca^{2+} regulation (35, 36); the ELC associates with the first IQ motif and is in contact with the motor domain, and the regulatory light chain adjoins the ELC and does not directly interact with the motor domain.

In conclusion, PK specifically cleaves myosin V at the neck region in the presence of Ca^{2+} , which produces BMV S-1 having intact IQ1 and IQ2. The IQ1 and IQ2 motifs

associate with CaM (not ELC), and high Ca^{2+} concentrations induce dissociation of CaM specifically from IQ2, which results in a loss of BMV motor function.

ACKNOWLEDGMENT

We thank Noriyuki Kodera and Yuta Saito for technical assistance.

REFERENCES

- Prekeris, R., and Terrian, D. M. (1997) Brain myosin V is a synaptic vesicle-associated motor protein: Evidence for a Ca^{2+} -dependent interaction with the synaptobrevin-synaptophysin complex, *J. Cell Biol.* 137, 1589–1601.
- Evans, L. L., Lee, A. J., Bridgman, P. C., and Mooseker, M. S. (1998) Vesicle-associated brain myosin-V can be activated to catalyze actin-based transport, *J. Cell Sci.* 111, 2055–2066.
- Tabb, S., Molyneaux, B. J., Cohen, D. L., Kuznetsov, S. A., and Langford, G. M. (1998) Transport of ER vesicles on actin filaments in neurons by myosin V, *J. Cell Sci.* 111, 3221–3234.
- Sakamoto, T., Amitani, I., Yokota, E., and Ando, T. (2000) Direct observation of processive movement by individual myosin V molecules, *Biochem. Biophys. Res. Commun.* 272, 586–590.
- De La Cruz, E. M., Wells, A. L., Rosenfeld, S. S., Ostap, E. M., and Sweeney, H. L. (1999) The kinetic mechanism of myosin V, *Proc. Natl. Acad. Sci. U.S.A.* 96, 13726–13731.
- Rosenfeld, S. S., and Sweeney, H. L. (2004) A model of myosin V processivity, *J. Biol. Chem.* 279, 40100–40111.
- Wang, F., Chen, L., Arcucci, O., Harvey, E. V., Bowers, B., Xu, Y., Hammer, J. A., and Sellers, J. R. (2000) Effect of ADP and ionic strength on the kinetic and motile properties of recombinant mouse myosin V, *J. Biol. Chem.* 275, 4329–4335.
- Mehta, A. D., Rock, R. S., Rief, M., Spudich, J. A., Mooseker, M. S., and Cheney, R. E. (1999) Myosin-V is a processive actin-based motor, *Nature* 400, 590–593.
- Rief, M., Rock, R. S., Mehta, A. D., Mooseker, M. S., Cheney, R. E., and Spudich, J. A. (2000) Myosin-V stepping kinetics: A molecular model for processivity, *Proc. Natl. Acad. Sci. U.S.A.* 97, 9482–9486.
- Mehta, A. D. (2001) Myosin learns to walk, *J. Cell Sci.* 114, 1981–1998.
- Yildiz, A., Forkey, J. N., McKinney, S. A., Ha, T., Goldman, Y. E., and Selvin, P. R. (2003) Myosin V walks hand-over-hand: Single fluorophore imaging with 1.5-nm localization, *Science* 300, 2061–2065.
- Forkey, J. N., Quinlan, M. E., Shaw, M. A., Corrie, J. E. T., and Goldman, Y. E. (2003) Three-dimensional structural dynamics of myosin V by single-molecule fluorescence polarization, *Nature* 422, 399–404.
- Cheney, R. E., O' Shea, M. K., Heuser, J. E., Coelho, M. V., Wolenski, J. S., Espreafico, E. M., Forscher, P., Larson, R. E., and Mooseker, M. S. (1993) Brain myosin-V is a two-headed unconventional myosin with motor activity, *Cell* 75, 13–23.
- Espindola, F. S., Suter, D. M., Partata, L. B., Cao, T., Wolenski, J. S., Cheney, R. E., King, S. M., and Mooseker, M. S. (2000) The light chain composition of chicken brain myosin-Va: Calmodulin, myosin-II essential light chains, and 8-kDa dynein light chain/PIN, *Cell Motil. Cytoskeleton* 47, 269–281.
- Espreafico, E. M., Cheney, R. E., Matteoli, M., Nascimento, A. A., De Camilli, P. V., Larson, R. E., and Mooseker, M. S. (1992) Primary structure and cellular localization of chicken brain myosin-V (p190), an unconventional myosin with calmodulin light chains, *J. Cell Biol.* 119, 1541–1557.
- Trybus, K. M., Kremensova, E., and Freyzon, Y. (1999) Kinetic characterization of a monomeric unconventional myosin V construct, *J. Biol. Chem.* 275, 27448–27456.
- Nascimento, A. A. C., Cheney, R. E., Tauhata, S. B. F., Larson, R. E., and Mooseker, M. S. (1996) Enzymatic characterization and functional domain mapping of brain myosin-V, *J. Biol. Chem.* 271, 17561–17569.
- Cameron, L. C., Carvalho, R. N., Araujo, J. R. V., Santos, A. C., Tauhata, S. B., Larson, R. E., and Sorenson, M. M. (1998) Calcium-induced quenching of intrinsic fluorescence in brain myosin V is linked to dissociation of calmodulin light chains, *Arch. Biochem. Biophys.* 355, 35–42.

19. Homma, K., Saito, J., Ikebe, R., and Ikebe, M. (2000) Ca^{2+} -dependent regulation of the motor activity of myosin V, *J. Biol. Chem.* 275, 34766–34771.
20. Nguyen, H., and Higuchi, H. (2005) Motility of myosin V regulated by the dissociation of single calmodulin, *Nat. Struct. Mol. Biol.* 12, 127–132.
21. Cheney, R. E. (1998) Purification and assay of myosin V, *Methods Enzymol.* 298, 3–18.
22. Kunioka, Y., and Ando, T. (1996) Innocuous labeling of the subfragment-2 region of skeletal muscle heavy meromyosin with a fluorescent polyacrylamide nanobead and visualization of individual heavy meromyosin molecules, *J. Biochem.* 119, 1024–1032.
23. Ando, T., Kodera, N., Takai, E., Maruyama, D., Saito, K., and Toda, A. (2001) A high-speed atomic force microscope for studying biological macromolecules, *Proc. Natl. Acad. Sci. U.S.A.* 98, 12468–12472.
24. Ando, T., Kodera, N., Naito, Y., Kinoshita, T., Furuta, K., and Toyoshima, Y. Y. (2003) A high-speed atomic force microscope for studying biological macromolecules in action, *Chem. Phys. Chem.* 4, 1196–1202.
25. Bayer, E. A., Ehrlich-Rogzinski, S., and Wilchek, M. (1996) Sodium dodecyl sulfate-polyacrylamide gel electrophoretic method for assessing the quaternary state and comparative thermostability of avidin and streptavidin, *Electrophoresis* 17, 1319–1324.
26. Manning, M., and Colon, W. (2004) Structural basis of protein kinetic stability: Resistance to sodium dodecyl sulfate suggests a central role for rigidity and a bias toward β -sheet structure, *Biochemistry* 43, 11248–11254.
27. Martin, S. R., and Bayley, P. M. (2002) Regulatory implications of a novel mode of interaction of calmodulin with a double IQ-motif target sequence from murine dilute myosin V, *Protein Sci.* 11, 2909–2923.
28. Martin, S. R., and Bayley, P. M. (2004) Calmodulin bridging of IQ motifs in myosin-V, *FEBS Lett.* 567, 166–170.
29. Kremontsov, D. N., Kremontsova, E. B., and Trybus, K. M. (2004) Myosin V: Regulation by calcium, calmodulin, and the tail domain, *J. Cell Biol.* 164, 877–886.
30. Sakamoto, T., Wang, F., Schmitz, S., Xu, Y., Xu, Q., Molloy, J. E., Veigel, C., and Sellers, J. R. (2003) Neck length and processivity of myosin V, *J. Biol. Chem.* 278, 29201–29207.
31. Sakamoto, T., Yildiz, A., Selvin, P. R., and Sellers, J. R. (2005) Step-size is determined by neck length in myosin V, *Biochemistry* 44, 16203–16210.
32. Yildiz, A., Forkey, J. N., McKinney, S. A., Ha, T., Goldman, Y. E., and Selvin, P. R. (2003) Myosin V walks hand-over-hand: Single fluorophore imaging with 1.5-nm localization, *Science* 300, 2061–2065.
33. De La Cruz, E. M., Wells, A. L., Sweeney, H. L., and Ostap, E. M. (2000) Actin and light chain isoform dependence of myosin V kinetics, *Biochemistry* 39, 14196–14202.
34. Coureux, P.-D., Wells, A. L., Menetrey, J., Yengo, C. M., Morris, C. A., Sweeney, H. L., and Houdusse, A. (2003) *Nature* 425, 419–423.
35. Xie, X., Harrison, D. H., Schlichting, I., Sweet, R. M., Kalabokis, V. N., Szent-Györgyi, A. G., and Cohen, C. (1994) Structure of the regulatory domain of scallop myosin at 2.8 Å resolution, *Nature* 368, 306–312.
36. Houdusse, A., and Cohen, C. (1995) Target sequence recognition by the calmodulin superfamily: Implications from light chain binding to the regulatory domain of scallop myosin, *Proc. Natl. Acad. Sci. U.S.A.* 92, 10644–10647.

BI0613877